Modeling the Pancreatic α-Cell: Dual Mechanisms of Glucose Suppression of Glucagon Secretion

Margaret Watts and Arthur Sherman*
Laboratory of Biological Modeling, National Institute of Diabetes and Digestive and Kidney Diseases, National Institutes of Health, Bethesda, Maryland

ABSTRACT The mechanism by which glucose induces insulin secretion in β-cells is fairly well understood. Despite years of research, however, the mechanism of glucagon secretion in α-cells is still not well established. It has been proposed that glucose regulates glucagon secretion by decreasing the conductance of either outward ATP-dependent potassium channels (K(ATP)) or an inward store-operated current (SOC). We have developed a mathematical model based on mouse data to test these hypotheses and found that both mechanisms are possible. Glucose metabolism closes K(ATP) channels, which depolarizes the cell but paradoxically reduces calcium influx by inactivating voltage-dependent calcium and sodium channels and decreases secretion. Glucose metabolism also activates SERCA pumps, which fills the endoplasmic reticulum and hyperpolarizes the cells by reducing the inward current through SOC channels and again suppresses glucagon secretion. We find further that the two mechanisms can combine to account for the nonmonotonic dependence of secretion on glucose observed in some studies, an effect that cannot be obtained with either mechanism alone.

INTRODUCTION

Glucose homeostasis is largely controlled by α- and β-cells located in pancreatic islets. Both cell types respond to blood glucose levels, albeit in an opposite manner. Whereas β-cells secrete insulin when blood glucose is elevated, α-cells secrete glucagon when blood glucose levels are low. The mechanism by which glucose induces insulin secretion in β-cells is fairly well understood. Glucose enters the cell through GLUT2 transporters, which causes an increase in the ATP/ADP ratio. This causes the ATP-sensitive K^+ (K(ATP)) channels to close, depolarizing the cell and allowing Ca^{2+} to enter through voltage-gated Ca^{2+} channels. This influx of Ca^{2+} triggers insulin secretion (1). Surprisingly, α-cells share much of the same secretory machinery as β-cells, including glucose transporters, voltage-gated Ca^{2+} channels, and K(ATP) channels. However, despite years of research, the mechanism of glucagon secretion is still not well understood (2).

There is an ongoing debate as to whether glucose suppresses glucagon secretion directly through an intrinsic mechanism, within the α-cell, or indirectly through an extrinsic mechanism (3). Although there is evidence that glucagon secretion is suppressed by paracrine effects such as insulin (4,5), Zn^+ (6,7), γ-amino butyric acid (8–10), and somatostatin (11–13), glucagon secretion in mice is maximally suppressed at glucose concentrations that are too low to stimulate insulin or somatostatin release (3,14). It has also been shown that paracrine regulators do not inhibit secretion below the basal rate (2). These facts point to a role for intrinsic regulation of glucagon secretion for low glucose concentrations (<6 or 7 mM) in mouse, but in humans the case is not so clear (3). Interspecies differences could account for some of the variation in data in the literature.

There are two theories for how glucose can intrinsically regulate glucagon secretion in the α-cell. One theory is that glucose affects the α-cell through closure of K(ATP) channels (15–17). As in β-cells, after glucose enters the cell, the ATP/ADP ratio would increase, leading to the closure of K(ATP) channels and cell depolarization. However, unlike β-cells, this depolarization has been proposed to decrease glucagon secretion. An alternative theory, which does not depend on K(ATP) channels, proposes that glucose regulates glucagon secretion through a store-operated current (SOC) (18,19). Glucose could regulate secretion through SOC by providing additional ATP to activate sarcoendoplasmic reticulum calcium transport ATPase (SERCA), which pumps and fill the Ca^{2+} stores. When glucose is high, the stores would fill, turning off SOC. The loss of current would reduce spike activity and decrease secretion. When glucose is low, Ca^{2+} stores would empty, turning on SOC and increasing spike activity and glucagon secretion.

In this article, we investigate how glucose can intrinsically regulate glucagon secretion by incorporating the effects of glucose on K(ATP) conductance ($g_{K(ATP)}$) and SOC (g_{SOC}) into a mathematical model for α-cell electrical activity and Ca^{2+} handling. We show that, depending upon the parameters of the cell, glucose can suppress glucagon secretion through either mechanism. We find further that the two mechanisms can combine to account for the nonmonotonic dependence of secretion on glucose observed in some studies, an effect that cannot be obtained with either mechanism alone. The model is mostly based on data from mouse, but we believe the basic principles would apply to humans because

Submitted August 19, 2013, and accepted for publication November 26, 2013.

*Correspondence: artiesherman@gmail.com

Editor: James Sneyd.

© 2014 by the Biophysical Society

0006-3495/14/02/0741/11 $2.00

http://dx.doi.org/10.1016/j.bpj.2013.11.4504

many of the mechanisms are shared. However, many of the results depend on quantitative relationships among parameters that differ in humans and mice, and they may not hold in humans even if they are correct for mice.

MATERIALS AND METHODS

Model

The model presented here is modified from a model of electrical activity in mouse α-cells (20). We add equations for cytosolic Ca^{2+}, endoplasmic reticulum (ER) Ca^{2+}, and secretion. We also modified parameters of the ionic currents to reduce spike frequency near threshold and increase spike amplitude, in better agreement with experimental data. In this section, we introduce the main features of the model. Equations and parameters not described here can be found in the Appendix, found in the Supporting Material. The original parameters from Diderichsen and Göpel (20) have been included in Table S1 and Table S2 in the Supporting Material for comparison. The equation for the plasma membrane potential (V) is

$$\frac{dV}{dt} = -\left(I_{\mathrm{CaL}} + I_{\mathrm{CaN}} + I_{\mathrm{CaT}} + I_{\mathrm{Na}} + I_{\mathrm{K}} + I_{\mathrm{K(ATP)}} + I_{\mathrm{KA}} + I_{\mathrm{L}} + I_{\mathrm{SOC}}\right)/C_m, \quad (1)$$

where C_m is the membrane capacitance; I_{CaL}, I_{CaN}, and I_{CaT} are L-, N-, and T-type voltage-dependent Ca^{2+} currents, respectively; I_{Na} is a voltage-dependent Na^+ current; I_{K} is a delayed rectifier K^+ current; I_{KA} is an A-type voltage-dependent K^+ current; $I_{\mathrm{K(ATP)}}$ is an ATP-sensitive K^+ current; I_L is a leak current; and I_{SOC} is a store-operated Ca^{2+} current.

The equation for $I_{\mathrm{K(ATP)}}$ is

$$I_{\mathrm{K(ATP)}} = g_{\mathrm{K(ATP)}}(V - V_K), \quad (2)$$

where $g_{\mathrm{K(ATP)}}$ is the K(ATP) channel conductance. To focus on the electrical properties of α-cells in this study, we do not consider glucose metabolism or the dependence of $g_{\mathrm{K(ATP)}}$ on the ATP/ADP ratio, but simply treat $g_{\mathrm{K(ATP)}}$ as a parameter that can be decreased to represent an increase in glucose or addition of a blocker, such as tolbutamide. The equation for I_{SOC} is

$$I_{\mathrm{SOC}} = \overline{g}_{\mathrm{soc}} c_{\mathrm{er}\infty}(V - V_{\mathrm{SOC}}), \quad (3)$$

where $\overline{g}_{\mathrm{SOC}}$ is the maximal conductance of the store-operated current, V_K and V_{SOC} are reversal potentials, and $c_{\mathrm{er}\infty}$ represents C_{er}-dependent activation, given by

$$c_{\mathrm{er}\infty}(C_{\mathrm{er}}) = \frac{1}{1 + \exp((C_{\mathrm{er}} - \overline{c}_{\mathrm{er}})/20)}. \quad (4)$$

Thus, the amount of calcium in the ER determines the amount of SOC current. Glucose can affect both $I_{\mathrm{K(ATP)}}$ and I_{SOC}. Glucose metabolism increases the ATP/ADP ratio, which decreases $g_{\mathrm{K(ATP)}}$. Glucose metabolism also fills the stores by activating SERCA pumps, which decreases the conductance of the SOC current, g_{SOC}, where

$$g_{\mathrm{SOC}} = \overline{g}_{\mathrm{SOC}}\, c_{\mathrm{er}\infty}(C_{\mathrm{er}}). \quad (5)$$

For glucose that is high enough, $I_{\mathrm{SOC}} \approx 0$.

In the absence of data on SOC in α-cells, we have modeled it as a nonselective cation current that carries Na^+ but not much Ca^{2+}, as reported in β-cells (21,22).

The original Diderichsen model did not include N-type Ca^{2+} channels, the SOC, Ca^{2+} dynamics, or glucagon secretion. Therefore, equations were added for bulk intracellular Ca^{2+} (C_i), Ca^{2+} in the endoplasmic reticulum (C_{er}), Ca^{2+} in a microdomain surrounding L- and N-type Ca^{2+} channels (C_{mdL}, C_{mdN}), and glucagon secretion.

Although Ca^{2+} enters mainly through L-type channels (18,23), N-type (15,16,24–26) and P/Q-type (27,28) channels have been suggested to be more important for glucagon secretion. We modeled glucagon secretion as depending on Ca^{2+} in the microdomains surrounding N-type Ca^{2+} channels, but our results would not change much if we had used P/Q channels because the main requirement is a high threshold for voltage activation. The rate of secretion is expressed as

$$J_{GS} = N_N\, m_{\mathrm{CaN}}\, h_{\mathrm{CaN}} \left(\frac{C_{\mathrm{mdN}}}{k_N + C_{\mathrm{mdN}}}\right)^4, \quad (6)$$

following the formulation in Pedersen and Sherman (29).

The total amount of glucagon secreted can be evaluated as

$$M_G = \int_0^t J_{GS} dt'. \quad (7)$$

The average glucagon secretion rate (GSR) plotted in the figures is calculated with an integral like that above, but with a 15-s moving time window.

The differential equations were solved numerically with the variable step size method CVODE implemented in the XPPAUT software package (30) with absolute and relative tolerances 10^{-10}.

RESULTS

Suppression of glucagon secretion through K(ATP) channels

The model produces action potentials (APs) with low frequency (~3 Hz) consistent with the experimental data obtained in low glucose (Fig. 1 *A*). The development of the individual currents during a single AP (Fig. 1 *B*) is shown in Fig. 1 *C*. T-type Ca^{2+} channels (not shown) are involved in the pacemaking of the APs. They open during the interspike interval before the onset of an AP. As the voltage slowly starts to rise, L-type channels begin to open. Then, the Na^+ current, I_{Na} (*solid curve*), activates causing the upstroke in the AP. After the membrane potential rises sufficiently, the L-type Ca^{2+} channel opens further along with N-type Ca^{2+} channels. I_{CaL} and I_{CaN} (*shaded* and *dashed shaded curves*, respectively) also contribute to the upstroke of the AP. Then the Na^+ current inactivates, and the delayed rectifier current, I_{K} (*dashed darker curve*), turns on, which together repolarize the cell. Like the T-type Ca^{2+} current, the A-type K^+ current, I_{KA} (not shown) also affects the interspike interval. The second bump in I_{Na} is due to Na^+ channels de-inactivating and was also seen in the original Diderichsen model.

To determine if K(ATP) channels or SOC can reduce glucagon secretion with the addition of glucose, we consider each mechanism separately. To begin, suppression of secretion by K(ATP) channels is explored by suppressing the dependence of SOC on C_{er} and setting the conductance of the SOC current (g_{SOC}) to a constant (0.2 nS). With g_{SOC}

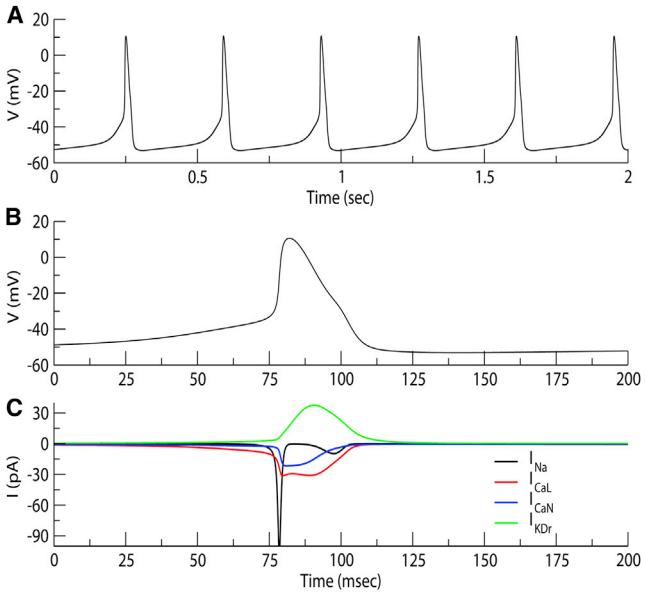

FIGURE 1 Electrical activity produced with the model. (*A*) Simulated α-cell spiking with the model in low glucose ($g_{K(ATP)} = 0.295$ nS and $\bar{g}_{SOC} = 0$ nS). (*B* and *C*) Simulated currents during a single action potential. I_{Na} triggers the sharp upstroke, leading to the activation of I_{CaL} and I_{CaN}. I_K repolarizes the cell. To see this figure in color, go online.

thus treated as a parameter of the system, the equation for the SOC current (Eq. 5) becomes

$$I_{SOC} = g_{SOC}(V - V_{SOC}). \quad (8)$$

It has been shown experimentally that adding glucose to a spiking α-cell can cause the cell to depolarize and produce spikes of reduced amplitude (15). These experiments are modeled by reducing $g_{K(ATP)}$ (Fig. 2). In the absence of glucose we assume that $g_{K(ATP)} = 0.32$ nS, and at this value the model cell spikes (Fig. 2 *A*). The large spikes bring in Ca^{2+}, raising C_i (Fig. 2 *B*) and increasing GSR (Fig. 2 *C*). We model the increase of glucose as a decrease in $g_{K(ATP)}$ (reduced ~17%, in line with Gromada et al. (15), to 0.265 nS). Now the cell produces spikes with a reduced amplitude, which reduces C_i and microdomain Ca^{2+}, C_{mdN} (not shown), due to inactivation of Ca^{2+} channels. As a consequence, glucagon secretion is reduced. When glucose is removed, the system reverts to the original large-amplitude spiking. Note that even though the reduction in amplitude is slight, there is a large effect on glucagon secretion.

By treating $g_{K(ATP)}$ as a parameter, we can construct a bifurcation diagram to show the behavior of the system as $g_{K(ATP)}$ is varied (Fig. 3 *A*). The solid curve represents the stable stationary solutions, and the dashed part the unstable solutions. As $g_{K(ATP)}$ is increased past a lower threshold, periodic solutions representing APs emerge (*solid circles*); the minimum and maximum voltages are plotted as an

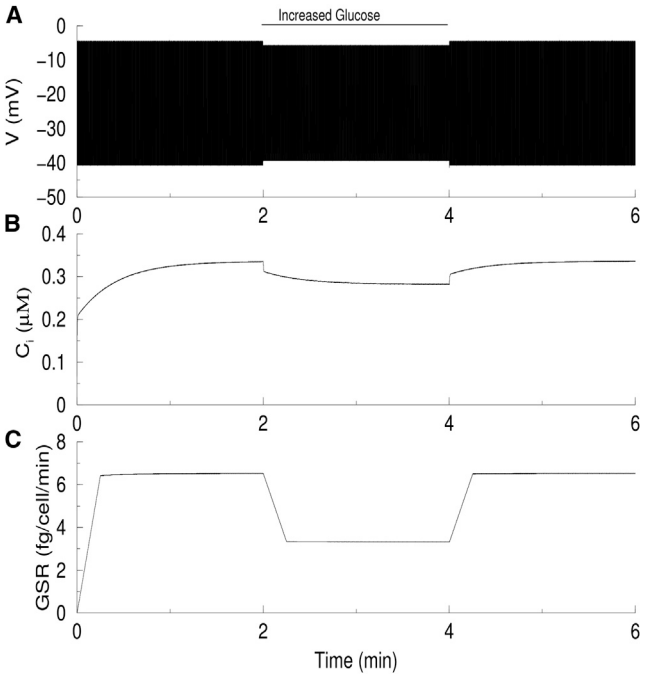

FIGURE 2 Glucose can suppress glucagon secretion by reducing $g_{K(ATP)}$ ($g_{SOC} = 0.2$ nS). (*A*) If we assume that $g_{K(ATP)} = 0.32$ nS in low glucose, the cell spikes and glucagon is secreted (*solid circle* in Fig. 3 *C*). Increasing glucose reduces $g_{K(ATP)}$, here set to 0.265 nS, reducing spike amplitude and Ca^{2+} entry. This decreases C_i (*B*), Ca^{2+} in the N-channel microdomains (not shown) and glucagon secretion (*C*, *blue circle* in Fig. 3 *C*).

indication of the amplitude. The threshold is mediated by a Hopf bifurcation (see Rinzel and Ermentrout (31) for a tutorial). This branch of solutions terminates at an upper threshold, mediated by a saddle node of periodic orbits (SNP), which is the point where the periodic branch from the left Hopf bifurcation intersects a branch of unstable periodic solutions (*open circles*) arising from a second Hopf bifurcation on the right. When $g_{K(ATP)}$ lies to the right of the SNP (i.e., is >~0.4 nS), the cell is hyperpolarized and silent.

We need not be concerned with the underlying mathematics but can just take the bifurcation diagram as a summary of the repertoire of cell behaviors. Starting on the right, as $g_{K(ATP)}$ is decreased, large-amplitude APs are produced, whereas further decreases in $g_{K(ATP)}$ decrease the amplitude because of inactivation of Na^+ and Ca^{2+} channels. There is also a small range of $g_{K(ATP)}$ values where the cell produces small-amplitude, depolarized spikes.

For $g_{K(ATP)}$ between ~0.18 and 0.26 nS, no stable steady states or periodic solutions are indicated in Fig. 3. In this region, patterns that are more complex are seen, such as spike doublets and a form of bursting. For simplicity, we have not labeled these and consider only ordinary spiking.

The electrical activity of the cell determines the amount of glucagon that is secreted. Fig. 3 *B* shows how changing $g_{K(ATP)}$ affects the amount of Ca^{2+} in the microdomain.

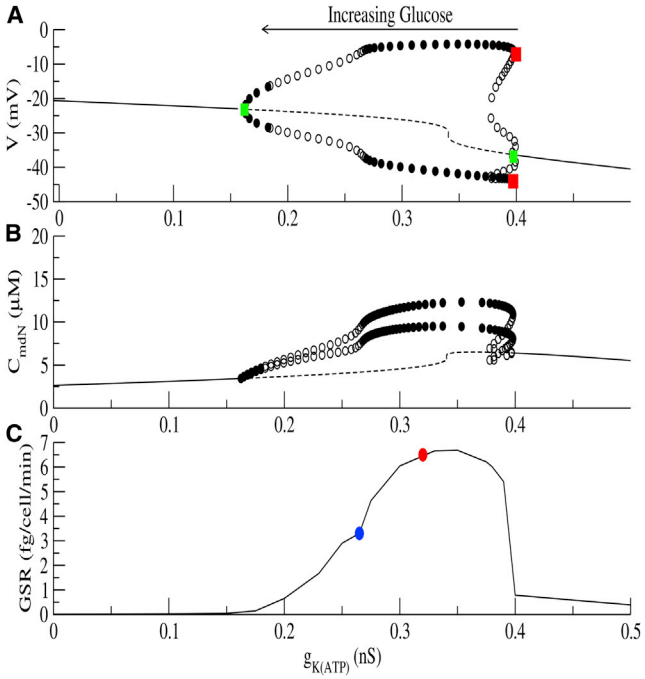

FIGURE 3 Bifurcation analysis of the model to investigate the role of $g_{K(ATP)}$. (*A*) Bifurcation diagram of the model with $g_{K(ATP)}$ as the bifurcation parameter ($g_{SOC} = 0.2$ nS). (*Solid curve*) Stable steady states; (*solid circles*) stable spiking solutions. Maximum and minimum voltages of the spike are plotted. (*Dashed curve*) Unstable steady states; (*open circles*) unstable periodic solutions. (*Green squares*) Hopf bifurcations; (*red squares*) saddle node of periodic bifurcations. (*B*) C_{mdN} first increases and then decreases as $g_{K(ATP)}$ decreases. (*C*) As $g_{K(ATP)}$ decreases, glucagon secretion rate (GSR) first increases, then decreases as a result of changes in spike frequency and C_{mdN}. (*Circles*) Low glucose (*red*) and high glucose (*blue*) conditions in Fig. 2, demonstrating that glucose can decrease glucagon secretion by decreasing $g_{K(ATP)}$. To see this figure in color, go online.

Fig. 3 *C* shows that as $g_{K(ATP)}$ decreases, the glucagon secretion rate (GSR) first increases and then decreases, producing a bell-shaped curve. Glucagon secretion depends on two features of the spikes, frequency and amplitude. GSR first increases as $g_{K(ATP)}$ decreases because the frequency increases, but then it decreases because amplitude decreases. Even a modest decrease in spike height leads to a significant decrease in secretion because the high-voltage activated N-type Ca^{2+} channels close, reducing Ca^{2+} in their microdomains. In Fig. 2, we showed that glucose reduced secretion by reducing spike amplitude. The bifurcation diagram in Fig. 3 predicts that a deeper reduction of $g_{K(ATP)}$ would produce smaller-amplitude spikes and a greater reduction in secretion. This corresponds to the behavior seen experimentally with the addition of tolbutamide (3,32). The results also agree with the relationship between glucagon secretion and K(ATP) channel activity seen in experiments using diazoxide (Dz) to titrate K(ATP) channel activity (3,16,17,33).

If we choose the solid circle (Fig. 3 *C*) to represent low glucose, and the shaded circle to represent high glucose, then glucose suppresses glucagon secretion at the same time that it depolarizes the cell. These correspond to the low and high glucose conditions in Fig. 2. However, we emphasize that, depending on the K(ATP) channel conductance at a particular glucose level, increasing glucose concentration could either increase or decrease glucagon secretion. Thus, we have shown that glucose can regulate glucagon secretion appropriately through its effect on $g_{K(ATP)}$, but that this is not guaranteed to work.

Suppression of glucagon secretion through a store-operated current

Next, we investigate suppression of glucagon secretion by an SOC, as suggested by the experiments in Liu et al. (18) and Vieira et al. (19). Store-operated current (SOC) is an inward current that decreases as ER Ca^{2+} increases, with conductance described by Eq. 5. Following Liu et al. (18) and Vieira et al. (19), we propose that in low glucose the store is relatively depleted because of limited SERCA activation, and the α-cell spikes. Increasing glucose activates SERCA and fills the ER, which turns off SOC and reduces secretion.

To investigate whether SOC can regulate glucagon secretion independently of K(ATP) channel activity, we fixed $g_{K(ATP)}$. In the absence of information about the relationship between glucose and SERCA activity in α-cells, we investigated the effects of changing k_{SERCA} (Fig. 4 *D*) on spiking and secretion through its effects on g_{SOC}. The value g_{SOC} was assumed to vary between 0 and 0.1 nS as C_{er} varies, a range sufficient to produce significant changes in spike activity.

Fig. 4 demonstrates regulation of glucagon secretion by this mechanism. In low glucose, the ER is depleted (Fig. 4 *C*), and g_{SOC} is ~0.075 nS (Fig. 4 *E*). Spiking drives Ca^{2+} entry, and glucagon is secreted (Fig. 4, *A*, *B*, and *F*). After increasing glucose, C_{er} increases, and g_{SOC} is reduced. The loss of current hyperpolarizes the cell, which suppresses Ca^{2+} entry and glucagon secretion. Note that C_{er} increases in this simulation because k_{SERCA} increases (Fig. 4 *D*), despite the reduction of C_i due to the loss of spiking. It was shown in Tengholm et al. (34) that the ER can fill even when cytosolic Ca^{2+} is low, provided sufficient ATP is present.

As we did for K(ATP) channels, we use a bifurcation diagram to examine the behavior of the system as a function of g_{SOC} (Fig. 5 *A*). The dependence of g_{SOC} on C_{er} and k_{SERCA} is not relevant for understanding the effect of SOC on membrane potential and C_{mdN}, so I_{SOC} is given by Eq. 8 as in Fig. 3, but now $g_{K(ATP)}$ is held fixed and g_{SOC} is varied. This diagram is roughly a mirror image of the one for $g_{K(ATP)}$ because SOC is an inward current. As g_{SOC} decreases, corresponding to increased glucose, the system goes from a depolarized steady state to small-amplitude APs to large-amplitude spikes to a low-voltage steady state, and C_{mdN} increases, then decreases. As for $g_{K(ATP)}$, GSR is

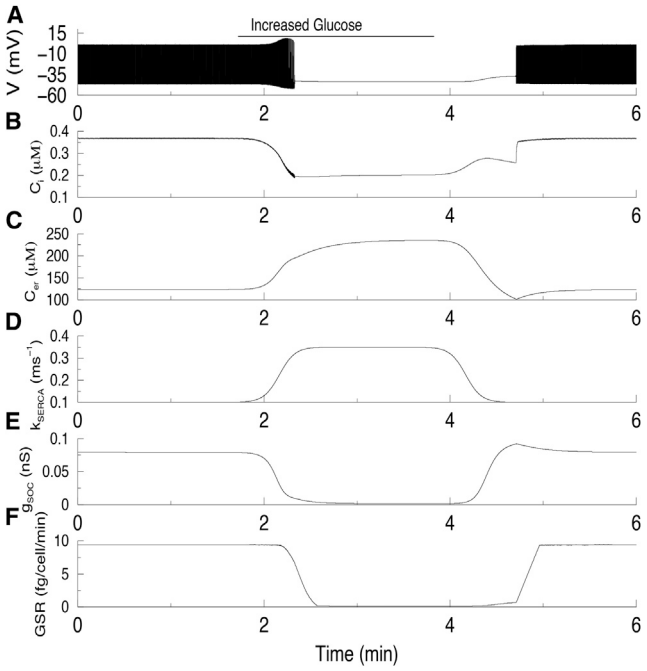

FIGURE 4 Glucose can suppress glucagon secretion by reducing g_{SOC}. (*A*) In the absence of glucose, $g_{K(ATP)}$ is set to 0.31 nS and k_{SERCA} to 0.1 ms^{-1}, resulting in $g_{SOC} \approx 0.075$ nS. The cell spikes and glucagon is secreted (*solid circle* in Fig. 5 *B*). Adding glucose hyperpolarizes the cell, which reduces C_i (*B*). Despite the reduction in C_i, the ER fills (*C*) because of the increase in k_{SERCA} (*D*). The changes in V and C_i (*E*) are driven by the reduction in g_{SOC}. (*F*) The hyperpolarization of V reduces C_{mdN} (not shown), which is responsible for the reduction in glucagon secretion (*blue circle* in Fig. 5 *B*).

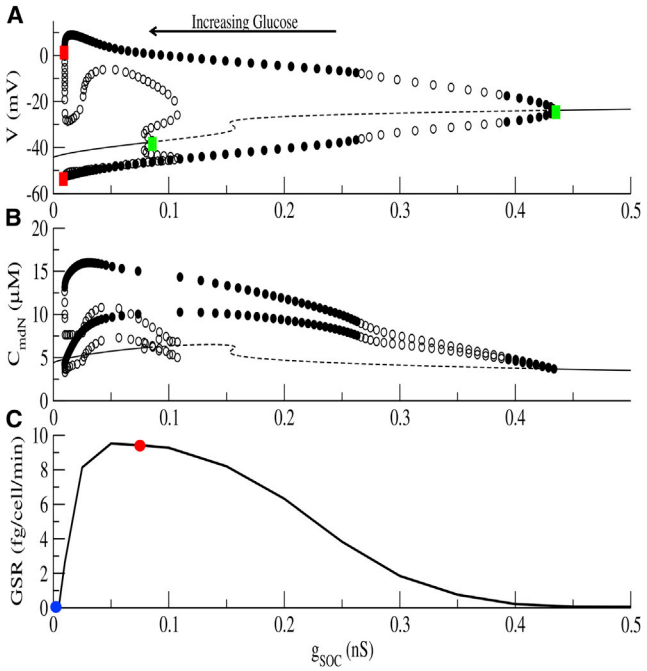

FIGURE 5 Bifurcation analysis of the model to investigate the role of SOC. (*A*) Bifurcation diagram of the model with g_{SOC} as the bifurcation parameter and $g_{K(ATP)}$ fixed at 0.31 nS. (*Green squares*) Hopf bifurcations; (*red squares*) saddle node of periodic bifurcations. (*B*) C_{mdN} increases and then decreases as g_{SOC} decreases. (*C*) GSR as a function of g_{SOC}. As g_{SOC} increases, the GSR first increases then decreases. (*Circles*) Low glucose (*red*) and high glucose (*blue*) conditions in Fig. 4, demonstrating that glucose can decrease glucagon secretion by decreasing g_{SOC}. To see this figure in color, go online.

determined by both the amplitude and frequency of spiking and again results in a bell-shaped curve. Thus, glucose can either increase or decrease glucagon secretion, depending on the level of g_{SOC} that corresponds to low glucose. The solid circle (Fig. 5 *C*) represents the low glucose condition in Fig. 4, whereas the shaded circle represents the high glucose condition. With these choices, increasing glucose decreases GSR.

Nonmonotonic glucose dose-response curve

Although it is possible to reduce glucagon secretion by either the K(ATP) channel or the SOC mechanism, it has been reported that glucagon secretion is maximally inhibited around 7 mM glucose (G), then increases as glucose levels rise further (3,14,19). Within the framework of our model, this *J*-shaped dose-response curve, with paradoxical stimulation of glucagon secretion at high glucose, cannot be modeled by changes in $g_{K(ATP)}$ or g_{SOC} alone. From Figs. 3 *C* and 5 *C* it can be seen that an increase in glucose will cause either a monotonic decrease in secretion or an increase followed by a decrease, depending on which point on the bell-shaped curve corresponds to low glucose. Although neither of these mechanisms alone can produce a decrease in secretion followed by an increase, we show in Fig. 6 that this result can be obtained by combining the effects of $g_{K(ATP)}$ and SOC.

Fig. 6 *A* is a two-parameter bifurcation diagram for the model, with $g_{K(ATP)}$ and g_{SOC} as the bifurcation parameters. It shows how the key bifurcations, with respect to $g_{K(ATP)}$ in Fig. 3 *A*, shift as g_{SOC} is varied. The left and right Hopf bifurcations (*solid curves* HB_L and HB_R), where the steady state gives way to spiking, slant up and to the right because more inhibition from $g_{K(ATP)}$ is needed to balance the increased inward SOC current. The shaded curve of SNPs, which marks the upper limit of spiking as $g_{K(ATP)}$ is increased, also generally slants to the right. We assume that increasing glucose will decrease both $g_{K(ATP)}$ and g_{SOC} as it blocks K(ATP) channels and increases SERCA activity, indicated by the arrow slanting down and to the left. If we further assume that SERCA activation is more sensitive to glucose metabolism than K(ATP) conductance, then g_{SOC} would decrease before $g_{K(ATP)}$ decreases. This implies a trajectory like the dashed curve. (See the Discussion for more on this point.)

Taking the parameters from the dashed curve (Fig. 6 *A*) produces a *J*-shaped glucose dose-response curve (Fig. 6 *B*), where the shaded circle represents low glucose, the solid

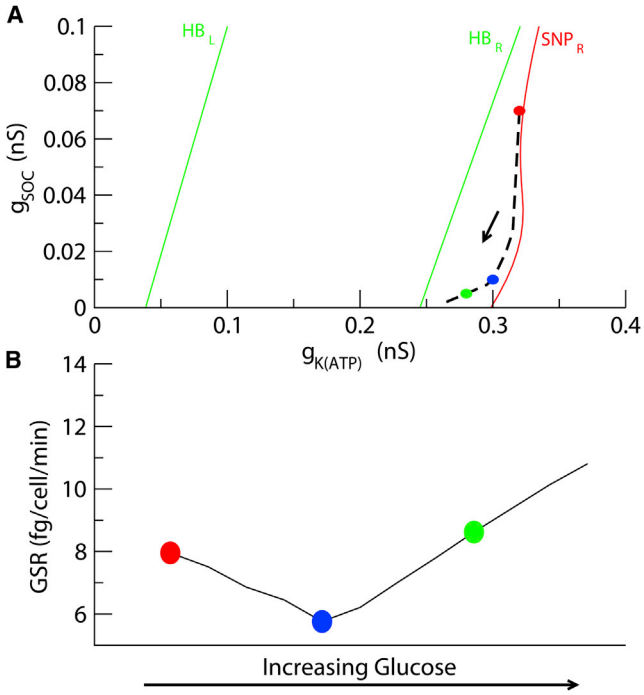

FIGURE 6 The model is able to produce a *J*-shaped glucose dose-response curve by combining the effects of $g_{K(ATP)}$ and SOC. (*A*) Two-parameter bifurcation diagram with $g_{K(ATP)}$ and g_{SOC} as the bifurcation parameters. If we assume that as glucose decreases, the phase point (*dashed line*) travels down (*arrow*), the model produces the dose-response curve in panel *B*. If the cell moves as shown (*red circle* to the *blue circle*), GSR decreases, mainly because of decreased g_{SOC}. As the cell moves from the *blue circle* to the *green circle*, GSR rises, mainly because of decreased $g_{K(ATP)}$. To see this figure in color, go online.

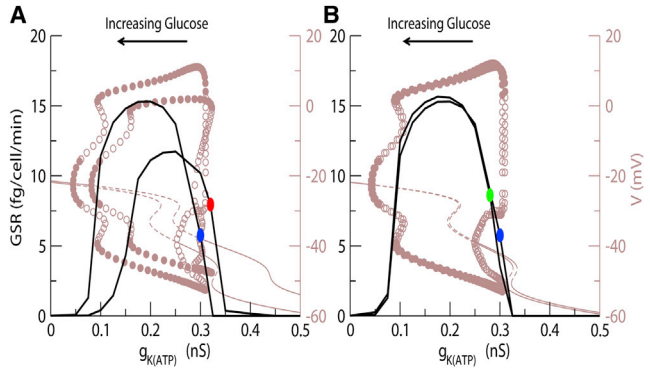

FIGURE 7 Bifurcation analysis reproducing the glucose dose-response curve. Bifurcation diagrams (*brown*) and glucagon secretion rate curves (*black*) are plotted for different values of g_{SOC}. (*A*) As g_{SOC} decreases, the bifurcation diagram moves to the left. Therefore, if low glucose conditions place the parameters as shown (*red circle*, $g_{SOC} = 0.07$), adding glucose will decrease g_{SOC} and $g_{K(ATP)}$. The net effect is a decrease in secretion (*blue circle*, $g_{SOC} = 0.01$). (*B*) If we now add more glucose to the system, g_{SOC} still decreases (but not as much), so the effect on the bifurcation diagram is reduced. Now, the net effect is an increase in secretion (*green circle*, $g_{SOC} = 0.005$) because decreasing $g_{K(ATP)}$ moves the cell up the GSR curve. To see this figure in color, go online.

circle represents intermediate glucose, and the open circle represents high glucose. In this scenario, the decrease in secretion from low to intermediate glucose results mainly from decreased SOC conductance, and the increase in secretion from intermediate to high glucose results mainly from decreased K(ATP) conductance.

An alternative view of how the *J*-shaped dose-response curve comes about is shown in Fig. 7, where instead of a two-parameter bifurcation diagram, we show how the one-parameter bifurcation diagrams with respect to $g_{K(ATP)}$ (*shaded curves*) shift as g_{SOC} changes. The solid curves are the corresponding glucagon secretion rates. In low glucose, g_{SOC} and $g_{K(ATP)}$ are at their highest levels (*rightmost curves*, $g_{SOC} = 0.07$). Increasing glucose decreases g_{SOC} and $g_{K(ATP)}$ (*leftmost curves*, $g_{SOC} = 0.01$). The decrease in g_{SOC} causes the bifurcation diagram and the GSR curve to shift to the left (Fig. 7 *A*). Thus, despite the reduction in $g_{K(ATP)}$, which by itself would have increased GSR, the decrease in g_{SOC} dominates and results in a decrease in GSR (the cell moves from the *shaded* to the *solid circle*).

A further increase in glucose has little effect on g_{SOC}, because SERCA is assumed to be saturated, and hence has little effect on the bifurcation diagram and GSR curve (Fig. 7 *B*). The main effect is the decrease in $g_{K(ATP)}$, which increases secretion (the cell moves from the *solid* to the *open circle* ($g_{SOC} = 0.005$), climbing up the GSR curve).

The conclusion that the initial decrease in secretion is due to a reduction in SOC, while the increase at higher glucose can be attributed to changes in $g_{K(ATP)}$, is supported by experimental data in Vieira et al. (19). That study reported that activation of SOC by blocking the SERCA pump with cyclopiazonic acid (CPA) increases glucagon secretion and prevents the inhibitory effect of glucose.

The model can reproduce the main features of those experiments, as shown in Fig. 8, which replots the glucose dose-response curve from Fig. 6 *B* (*solid*) along with the glucose dose-response curve with CPA added (*dashed*). The addition of CPA was modeled by fixing g_{SOC} at 0.08 nS. As in the experiments, glucagon secretion is higher for all glucose levels in the presence of CPA, and the inhibitory effect of glucose has been lost.

Another recent article (35) demonstrates that glucose (G) and tolbutamide (Tolb) exert distinct effects on glucagon secretion. In fact, it was argued that there exists an unknown mechanism that contributes to glucose suppression of glucagon secretion other than K(ATP) channels and paracrine factors. We propose that the unknown mechanism is, at least in part, SOC.

One particular experiment in Cheng-Xue et al. (35) showed an inhibitory effect of Tolb in 1 mM (G), but a stimulatory effect in 7 mM G. The model can reproduce this data if we make certain assumptions about the SOC and K(ATP) conductances. We assume that SOC is on in low glucose, nominally 1 mM (Fig. 9, *A–C*). We further assume that the cell sits near the peak of the GSR curve. In this scenario,

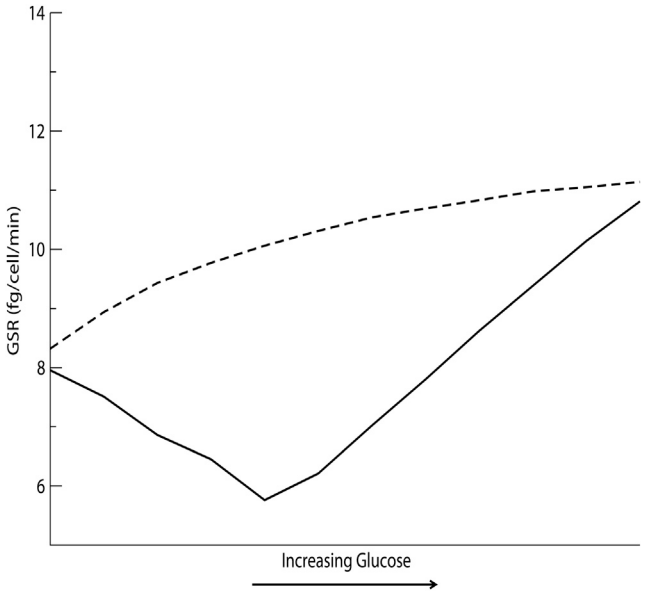

FIGURE 8 Effects of the SERCA inhibitor cyclopiazonic acid (CPA) on glucagon secretion. In the presence of CPA, g_{SOC} is set to 0.08 nS. Glucagon section is higher and the inhibitory effect of glucose has been lost (*dashed curve*). The glucose dose-response curve from Fig. 7 *B* (*solid curve*) is plotted for comparison.

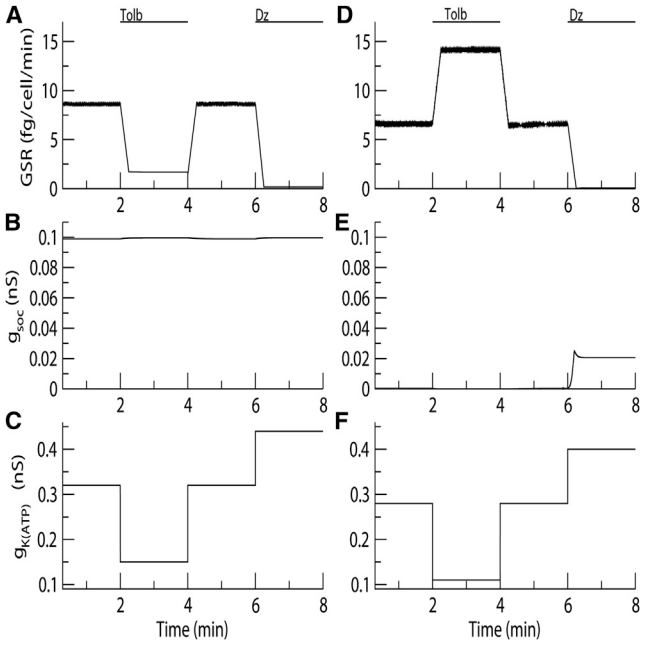

FIGURE 9 Effect of tolbutamide (Tolb) and diazoxide (Dz) for two different levels of glucose. (*A–C*) In low glucose, we assume $k_{SERCA} = 0.05\ ms^{-1}$, making $g_{SOC} = 0.1$ nS during the simulation. Reducing $g_{K(ATP)}$ with tolbutamide (Tolb) reduces Ca^{2+} entry and secretion is reduced. Opening K(ATP) channels with Dz increases $g_{K(ATP)}$ and decreases secretion. (*D–F*) In the presence of glucose, we assume $k_{SERCA} = 0.3\ ms^{-1}$, making $g_{SOC} = 0$ nS during the simulation. The addition of Tolb heightens secretion, whereas the addition of Dz decreases it.

the addition of tolbutamide would cause a reversible decrease in $g_{K(ATP)}$ and a reduction in secretion. The addition of Dz, which increases $g_{K(ATP)}$, would also reduce secretion.

However, in intermediate glucose, nominally 7 mM, SOC would be off because glucose would fill the ER, and $g_{K(ATP)}$ would be lower (Fig. 9, *D–F*). The net result would be a glucagon secretion rate lower than at 1 mM G (Fig. 9 *D*). Now the addition of Tolb increases secretion, whereas Dz still inhibits secretion. For the simulations in Fig. 9, the change in glucose concentrations modeled by a change in k_{SERCA} and $g_{K(ATP)}$, whereas the addition of tolbutamide only affects $g_{K(ATP)}$.

Fig. 10 shows the glucagon secretion rate curves corresponding to the simulations in Fig. 9 for low glucose ($g_{SOC} = 0.1$ nS; *dashed curve*) and intermediate glucose ($g_{SOC} = 0$; *solid curve*). In low glucose, the GSR curve lies to the right of the GSR curve in intermediate glucose because of the stimulus provided by SOC. In Fig. 9, *A–C*, $g_{K(ATP)}$ was chosen such that secretion was almost maximal (*open shaded circle*), so addition of Tolb decreased secretion (*open circle*). In Fig. 9, *D–F*, in contrast, we assumed that $g_{K(ATP)}$, while reduced, lay to the right of the maximum (*solid shaded circle*), so decreasing $g_{K(ATP)}$ with Tolb, increased secretion (*solid circle*).

Of course, if the decrease in $g_{K(ATP)}$ due to increased glucose had been great enough, Tolb would have decreased secretion. Nonetheless, there is a wide range of possible $g_{K(ATP)}$ values that would result in an increase. Conductances were not measured in Cheng-Xue et al. (35), so we can only say that the mechanism is plausible, not that it is proven. A further caveat is that the model does not yet address paracrine effects, which may also have contributed in the experiments.

DISCUSSION

We have described a mathematical model of the pancreatic α-cell and used it to demonstrate two separate mechanisms for intrinsic regulation of glucagon secretion. The first mechanism demonstrated was suppression of glucagon secretion by closure of K(ATP) channels (Fig. 2). This scenario assumes that glucose raises the ATP/ADP ratio. It is also necessary to assume that the prevailing K(ATP) channel conductance in low glucose lies near the maximum of the curve of glucagon secretion versus $g_{K(ATP)}$ (Fig. 3). Then, the depolarization due to reduced $g_{K(ATP)}$ would reduce spike amplitude, decrease Ca^{2+} influx through N-type Ca^{2+} channels and reduce glucagon secretion.

The effect of glucose on the ATP/ADP ratio in α-cells is uncertain. Some studies report no change (23,36), but others show an increase in ATP with glucose (6,37,38). We have sidestepped this by simulating the effect of changes in K(ATP) conductance rather than changes in ATP/ADP. Even if glucose does close K(ATP) channels in α-cells, secretion might not be inhibited. Some studies have shown that

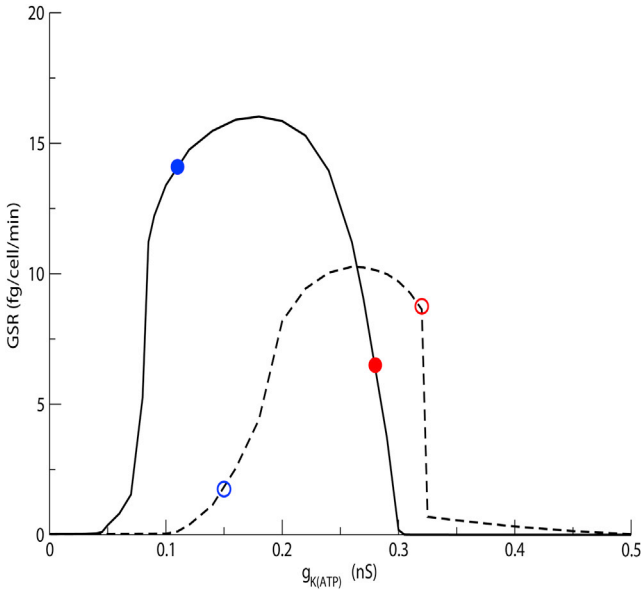

FIGURE 10 GSRs for the simulations in Fig. 9. In low glucose conditions (*dashed curve*), before Tolb was added, the parameters were as shown (*open red circle*), and glucagon secretion was near maximal. After Tolb was added, $g_{K(ATP)}$ decreased (*open blue circle*), and the glucagon secretion rate decreased. In intermediate glucose (*solid curve*), before Tolb was added (*solid red circle*) the parameters sat to the right of the maximal secretion point. Therefore when Tolb was added, secretion increased (*solid blue circle*). Note that the decrement in $g_{K(ATP)}$ assumed for Tolb was the same for both cases; only the position on the GSR curve differed. To see this figure in color, go online.

glucose stimulates glucagon secretion in isolated α-cells (6,39–41). Indeed, as we have emphasized, the model indicates that the effect of K(ATP) channel closure depends on the position of $g_{K(ATP)}$ along the GSR curve. Although the model may seem to be maddeningly inconclusive, we believe that it in fact reflects faithfully the maddeningly inconclusive data and is the only way to make sense of that data.

There is no getting around the fact that α-cells are extremely heterogeneous (42–44), and the bell-shaped GSR curves imply that quantitative variation can change the direction of an effect. The studies reporting that glucose stimulates glucagon secretion (6,39–41) have been used to argue that glucagon secretion is suppressed by paracrine, rather than intrinsic, factors. We return to this point at the end and posit a deep connection between heterogeneity and paracrine effects.

To make matters more complicated, we have shown that glucose can also suppress glucagon secretion by reducing an SOC (Fig. 4). This scenario assumes that the SOC and K(ATP) conductances in low glucose place the cell near the maximum of the GSR curve (Fig. 5). It further assumes that increased glucose metabolism activates SERCA pumps. Given this, glucose would fill the ER, reduce g_{SOC}, and hyperpolarize the cells. A recent article (35) suggests that something other than paracrine factors or K(ATP) channels is needed to explain the suppression of glucagon secretion by glucose. The model shows that SOC is well suited to fill this gap and is supported by data showing loss of suppression when the SERCA pump is blocked by CPA (19), an effect that can be simulated by the model (Fig. 8). We know even less about the effect of glucose on SOC than on K(ATP); indeed there is no direct electrophysiological evidence for the existence of SOC current in α-cells. We have sidestepped this by simulating the effects of changes in SERCA pump activity rather than glucose, but even this depends on unknown relationships among SERCA, ER Ca^{2+}, and SOC conductance. The surest thing we can say is that the two-parameter bifurcation diagram (Fig. 6 *A*) implies a constraint: the larger the K(ATP) conductance, the larger the SOC (or other inward) conductance needed to counterbalance it.

The electrical effects of the two mechanisms are opposite: K(ATP) depolarizes the cell and SOC hyperpolarizes it. That both depolarization and hyperpolarization can reduce secretion is a consequence of the bell-shaped GSR curves. For the same reason, they can both increase secretion. Experimentally it has been reported both that glucose depolarizes α-cells (7,15,17) and that it hyperpolarizes them (25,45). We propose that both K(ATP) channels and SOC are present and affect glucagon secretion in the α-cell, but the direction of the effect is determined by where a given cell sits on the GSR curves generated by the two conductances. Again, heterogeneity is key.

The most appealing model is one in which SOC and K(ATP) work together. Of the mechanisms we have considered, this combination, and only this combination, can account (Figs. 6–8) for the *J*-shaped secretion dose-response curve observed experimentally (3,14,19). In this scenario the reduction as glucose concentration is increased from, say, 1 to 7 mM is due to SOC and the paradoxical rise at higher glucose is due to K(ATP). It has been argued (41,46) that the increase in glucagon secretion at high glucose operates through a non-Ca^{2+}-dependent pathway, possibly increased granule mobilization, analogous to the amplification effect on insulin exocytosis in β-cells (1). Supporting this hypothesis, in Salehi et al. (14) an increase in glucose from 7 to 30 mM in the presence of diazoxide increased glucagon secretion in the absence of any change in Ca^{2+} concentration. This does not, however, rule out an increase also in Ca^{2+} concentration when Ca^{2+} is not clamped. Such an increase is shown in Le Marchand and Piston (41), and, unless Ca^{2+} is elevated at high glucose, there would not be much secretion for metabolism to amplify. The combination of SOC and K(ATP) assumed in Fig. 6 can also explain (Figs. 9 and 10) the opposite reactions to tolbutamide in 1 and 7 mM G reported in Cheng-Xue et al. (35).

The assumption that SERCA saturates at a lower glucose concentration than K(ATP) conductance is suggested by data from β-cells showing that the ER Ca^{2+} saturates at 8 mM glucose (47), whereas K(ATP) conductance continues to decrease as glucose is raised from 10 to 20 mM (48); we

do not have such information about α-cells. A *J*-shaped curve can also be obtained by assuming the opposite, that K(ATP) conductance saturates first (not shown) because the directions reverse on the opposite arms of the bell-shaped curves: When SOC conductance is large, decreasing K(ATP) conductance decreases secretion, and at low K(ATP) conductance, decreasing SOC conductance increases secretion. In this case, however, the flattening of the dose-response curve simulated in Fig. 8 would not occur.

The bell-shaped curves may also help explain the dysregulation of glucagon secretion in both Type-1 and Type-2 diabetes, in which too much glucagon is secreted at high glucose levels, while not enough glucagon is secreted at low glucose (49–54). The first effect could be attributed to diabetic α-cells having a slightly higher K(ATP) channel conductance. The cell would then sit on the right arm of the bell-shaped curve, and glucose would stimulate glucagon secretion rather than suppress it (3,33). A lack of paracrine insulin to suppress glucagon secretion likely also plays a role here. Indeed, a chronic deficit in exposure to insulin could possibly contribute to dysregulation of α-cell intrinsic mechanisms, such as excessive K(ATP) expression, in addition to loss of direct control by insulin.

A few other α-cell models have been previously published (20,55–57). These models differ quantitatively from ours, but those of Diderichsen and Göpel (20) and of Fridlyand and Philipson (57) also have bell-shaped dose-response curves, suggesting that this is a robust feature of α-cells. It should be possible to combine K(ATP) and SOC effects in those models, if one prefers them, and obtain results similar to ours.

A major limitation of our model, as well as its predecessors, is that it neglects paracrine effects. We have shown that, allowing certain assumptions, intrinsic effects are sufficient to account for the key features of the response of glucagon to glucose, which raises the question of what role paracrine effects play. We do not deny the importance of paracrine effects, but suggest that their role is different than previously proposed: to modulate the core intrinsic mechanisms and overcome the heterogeneity of the α-cells. Whereas β-cell heterogeneity is suppressed by gap junctional coupling, α-cells lack this mechanism. A dramatic indication of this is contained in two recent articles (41,46), which showed that the majority of α-cells in an islet increased cytosolic Ca^{2+} with glucose and only a minority exhibited decreased Ca^{2+}. We suggest that insulin and/or somatostatin could help suppress α-cells that inappropriately secrete at high glucose. We believe it is more likely that insulin and somatostatin are important at high glucose than at low glucose, where their secretion is low. We note as well that very few α-cells are needed to maintain proper glucagon secretion (58), so that the surviving minority would suffice.

Coupling also allows β-cells to secrete synchronously and generate whole-body pulsatility. Unpublished work by us indicates that paracrine effects can serve this function for α-cells as well. Indeed, at least some α-cells must be active at high glucose to account for the antisynchronous pulses of insulin and glucagon observed in elevated glucose (43,59,60). A full exploration of these issues requires a model islet with paracrine interactions among α-, β-, and δ-cells. We are currently working on such a model using the model presented here as a base.

SUPPORTING MATERIAL

An Appendix, comprising 20 Model Equations and three tables, is available at http://www.biophysj.org/biophysj/supplemental/S0006-3495(13)05843-8.

This work was supported by the Intramural Research Program of the National Institute of Diabetes and Digestive and Kidney Diseases, National Institutes of Health, Bethesda, MD.

REFERENCES

1. Henquin, J. C. 2000. Triggering and amplifying pathways of regulation of insulin secretion by glucose. *Diabetes.* 49:1751–1760.
2. Gromada, J., I. Franklin, and C. B. Wollheim. 2007. Alpha-cells of the endocrine pancreas: 35 years of research but the enigma remains. *Endocr. Rev.* 28:84–116.
3. Walker, J. N., R. Ramracheya, …, P. Rorsman. 2011. Regulation of glucagon secretion by glucose: paracrine, intrinsic or both? *Diabetes Obes. Metab.* 13 (*Suppl 1*):95–105.
4. Maruyama, H., A. Hisatomi, …, R. H. Unger. 1984. Insulin within islets is a physiologic glucagon release inhibitor. *J. Clin. Invest.* 74:2296–2299.
5. Samols, E., and J. I. Stagner. 1988. Intra-islet regulation. *Am. J. Med.* 85:31–35.
6. Ishihara, H., P. Maechler, …, C. B. Wollheim. 2003. Islet β-cell secretion determines glucagon release from neighboring α-cells. *Nat. Cell Biol.* 5:330–335.
7. Franklin, I., J. Gromada, …, C. B. Wollheim. 2005. Beta-cell secretory products activate α-cell ATP-dependent potassium channels to inhibit glucagon release. *Diabetes.* 54:1808–1815.
8. Franklin, I. K., and C. B. Wollheim. 2004. GABA in the endocrine pancreas: its putative role as an islet cell paracrine-signaling molecule. *J. Gen. Physiol.* 123:185–190.
9. Wendt, A., B. Birnir, …, M. Braun. 2004. Glucose inhibition of glucagon secretion from rat α-cells is mediated by GABA released from neighboring β-cells. *Diabetes.* 53:1038–1045.
10. Rorsman, P., P. O. Berggren, …, P. A. Smith. 1989. Glucose-inhibition of glucagon secretion involves activation of $GABA_A$-receptor chloride channels. *Nature.* 341:233–236.
11. Gerich, J. E., R. Lovinger, and G. M. Grodsky. 1975. Inhibition by somatostatin of glucagon and insulin release from the perfused rat pancreas in response to arginine, isoproterenol and theophylline: evidence for a preferential effect on glucagon secretion. *Endocrinology.* 96:749–754.
12. Strowski, M. Z., R. M. Parmar, …, J. M. Schaeffer. 2000. Somatostatin inhibits insulin and glucagon secretion via two receptors subtypes: an in vitro study of pancreatic islets from somatostatin receptor 2 knockout mice. *Endocrinology.* 141:111–117.
13. Hauge-Evans, A. C., A. J. King, …, P. M. Jones. 2009. Somatostatin secreted by islet δ-cells fulfills multiple roles as a paracrine regulator of islet function. *Diabetes.* 58:403–411.

14. Salehi, A., E. Vieira, and E. Gylfe. 2006. Paradoxical stimulation of glucagon secretion by high glucose concentrations. *Diabetes.* 55:2318–2323.
15. Gromada, J., X. Ma, …, P. Rorsman. 2004. ATP-sensitive K^+ channel-dependent regulation of glucagon release and electrical activity by glucose in wild-type and $SUR1^{-/-}$ mouse α-cells. *Diabetes.* 53 (*Suppl 3*):S181–S189.
16. MacDonald, P. E., Y. Z. De Marinis, …, P. Rorsman. 2007. A K(ATP) channel-dependent pathway within α cells regulates glucagon release from both rodent and human islets of Langerhans. *PLoS Biol.* 5:e143.
17. Göpel, S. O., T. Kanno, …, P. Rorsman. 2000. Regulation of glucagon release in mouse α-cells by K_{ATP} channels and inactivation of TTX-sensitive Na^+ channels. *J. Physiol.* 528:509–520.
18. Liu, Y. J., E. Vieira, and E. Gylfe. 2004. A store-operated mechanism determines the activity of the electrically excitable glucagon-secreting pancreatic α-cell. *Cell Calcium.* 35:357–365.
19. Vieira, E., A. Salehi, and E. Gylfe. 2007. Glucose inhibits glucagon secretion by a direct effect on mouse pancreatic alpha cells. *Diabetologia.* 50:370–379.
20. Diderichsen, P. M., and S. O. Göpel. 2006. Modeling the electrical activity of pancreatic α-cells based on experimental data from intact mouse islets. *J. Biol. Phys.* 32:209–229.
21. Worley, 3rd, J. F., M. S. McIntyre, …, I. D. Dukes. 1994. Depletion of intracellular Ca^{2+} stores activates a maitotoxin-sensitive nonselective cationic current in β-cells. *J. Biol. Chem.* 269:32055–32058.
22. Mears, D., and C. L. Zimliki. 2004. Muscarinic agonists activate Ca^{2+} store-operated and -independent ionic currents in insulin-secreting HIT-T15 cells and mouse pancreatic β-cells. *J. Membr. Biol.* 197:59–70.
23. Quoix, N., R. Cheng-Xue, …, P. Gilon. 2009. Glucose and pharmacological modulators of ATP-sensitive K^+ channels control $Ca^{2+}{}_c$ by different mechanisms in isolated mouse α-cells. *Diabetes.* 58:412–421.
24. Gromada, J., K. Bokvist, …, P. Rorsman. 1997. Adrenaline stimulates glucagon secretion in pancreatic A-cells by increasing the Ca^{2+} current and the number of granules close to the L-type Ca^{2+} channels. *J. Gen. Physiol.* 110:217–228.
25. Barg, S., J. Galvanovskis, …, L. Eliasson. 2000. Tight coupling between electrical activity and exocytosis in mouse glucagon-secreting α-cells. *Diabetes.* 49:1500–1510.
26. Göpel, S., Q. Zhang, …, P. Rorsman. 2004. Capacitance measurements of exocytosis in mouse pancreatic α-, β- and δ-cells within intact islets of Langerhans. *J. Physiol.* 556:711–726.
27. Vignali, S., V. Leiss, …, A. Welling. 2006. Characterization of voltage-dependent sodium and calcium channels in mouse pancreatic A- and B-cells. *J. Physiol.* 572:691–706.
28. Rorsman, P., M. Braun, and Q. Zhang. 2012. Regulation of calcium in pancreatic α- and β-cells in health and disease. *Cell Calcium.* 51:300–308.
29. Pedersen, M. G., and A. Sherman. 2009. Newcomer insulin secretory granules as a highly calcium-sensitive pool. *Proc. Natl. Acad. Sci. USA.* 106:7432–7436.
30. Ermentrout, B. 2002. Simulating, Analyzing, and Animating Dynamical Systems: A Guide to XPPAUT for Researchers and Students. SIAM, Philadelphia, PA.
31. Rinzel, J., and G. B. Ermentrout. 1998. Analysis of neural excitability and oscillations. *In* Methods in Neuronal Modeling: From Ions to Networks, 2nd. C. Koch and I. Segev, editors. MIT Press, Cambridge, MA, pp. 251–292.
32. Ramracheya, R., C. Ward, …, M. Braun. 2010. Membrane potential-dependent inactivation of voltage-gated ion channels in α-cells inhibits glucagon secretion from human islets. *Diabetes.* 59:2198–2208.
33. Rorsman, P., S. A. Salehi, …, P. E. MacDonald. 2008. K_{ATP}-channels and glucose-regulated glucagon secretion. *Trends Endocrinol. Metab.* 19:277–284.
34. Tengholm, A., B. Hellman, and E. Gylfe. 1999. Glucose regulation of free Ca^{2+} in the endoplasmic reticulum of mouse pancreatic β cells. *J. Biol. Chem.* 274:36883–36890.
35. Cheng-Xue, R., A. Gómez-Ruiz, …, P. Gilon. 2013. Tolbutamide controls glucagon release from mouse islets differently than glucose: involvement of K(ATP) channels from both α-cells and δ-cells. *Diabetes.* 62:1612–1622.
36. Detimary, P., S. Dejonghe, …, J. C. Henquin. 1998. The changes in adenine nucleotides measured in glucose-stimulated rodent islets occur in β cells but not in α cells and are also observed in human islets. *J. Biol. Chem.* 273:33905–33908.
37. Ravier, M. A., and G. A. Rutter. 2005. Glucose or insulin, but not zinc ions, inhibit glucagon secretion from mouse pancreatic α-cells. *Diabetes.* 54:1789–1797.
38. Leclerc, I., G. Sun, …, G. A. Rutter. 2011. AMP-activated protein kinase regulates glucagon secretion from mouse pancreatic α-cells. *Diabetologia.* 54:125–134.
39. Pipeleers, D. G., F. C. Schuit, …, M. van de Winkel. 1985. Interplay of nutrients and hormones in the regulation of glucagon release. *Endocrinology.* 117:817–823.
40. Olsen, H. L., S. Theander, …, J. Gromada. 2005. Glucose stimulates glucagon release in single rat α-cells by mechanisms that mirror the stimulus-secretion coupling in β-cells. *Endocrinology.* 146:4861–4870.
41. Le Marchand, S. J., and D. W. Piston. 2010. Glucose suppression of glucagon secretion: metabolic and calcium responses from α-cells in intact mouse pancreatic islets. *J. Biol. Chem.* 285:14389–14398.
42. Nadal, A., I. Quesada, and B. Soria. 1999. Homologous and heterologous asynchronicity between identified α-, β- and δ-cells within intact islets of Langerhans in the mouse. *J. Physiol.* 517:85–93.
43. Quesada, I., M. G. Todorova, …, B. Soria. 2006. Glucose induces opposite intracellular Ca^{2+} concentration oscillatory patterns in identified α- and β-cells within intact human islets of Langerhans. *Diabetes.* 55:2463–2469.
44. Huang, Y. C., M. Rupnik, and H. Y. Gaisano. 2011. Unperturbed islet α-cell function examined in mouse pancreas tissue slices. *J. Physiol.* 589:395–408.
45. Manning Fox, J. E., A. V. Gyulkhandanyan, …, M. B. Wheeler. 2006. Oscillatory membrane potential response to glucose in islet β-cells: a comparison of islet-cell electrical activity in mouse and rat. *Endocrinology.* 147:4655–4663.
46. Le Marchand, S. J., and D. W. Piston. 2012. Glucose decouples intracellular Ca^{2+} activity from glucagon secretion in mouse pancreatic islet α-cells. *PLoS ONE.* 7:e47084.
47. Ravier, M. A., D. Daro, …, P. Gilon. 2011. Mechanisms of control of the free Ca^{2+} concentration in the endoplasmic reticulum of mouse pancreatic β-cells: interplay with cell metabolism and $[Ca^{2+}]_c$ and role of SERCA2b and SERCA3. *Diabetes.* 60:2533–2545.
48. Tarasov, A. I., C. A. Girard, and F. M. Ashcroft. 2006. ATP sensitivity of the ATP-sensitive K^+ channel in intact and permeabilized pancreatic β-cells. *Diabetes.* 55:2446–2454.
49. Butler, P. C., and R. A. Rizza. 1991. Contribution to postprandial hyperglycemia and effect on initial splanchnic glucose clearance of hepatic glucose cycling in glucose-intolerant or NIDDM patients. *Diabetes.* 40:73–81.
50. Dunning, B. E., and J. E. Gerich. 2007. The role of α-cell dysregulation in fasting and postprandial hyperglycemia in type 2 diabetes and therapeutic implications. *Endocr. Rev.* 28:253–283.
51. Quesada, I., E. Tudurí, …, A. Nadal. 2008. Physiology of the pancreatic α-cell and glucagon secretion: role in glucose homeostasis and diabetes. *J. Endocrinol.* 199:5–19.
52. Cryer, P. E., S. N. Davis, and H. Shamoon. 2003. Hypoglycemia in diabetes. *Diabetes Care.* 26:1902–1912.
53. Unger, R. H., and L. Orci. 2010. Paracrinology of islets and the paracrinopathy of diabetes. *Proc. Natl. Acad. Sci. USA.* 107:16009–16012.
54. Cryer, P. E. 2008. Glucagon and hyperglycemia in diabetes. *Clin. Sci.* 114:589–590.
55. Gonzalez-Velez, V., A. Gil, and I. Quesada. 2010. Minimal state models for ionic channels involved in glucagon secretion. *Math. Biosci. Eng.* 7:793–807.

56. González-Vélez, V., G. Dupont, …, I. Quesada. 2012. Model for glucagon secretion by pancreatic α-cells. *PLoS ONE.* 7:e32282.

57. Fridlyand, L. E., and L. H. Philipson. 2012. A computational systems analysis of factors regulating α-cell glucagon secretion. *Islets.* 4:262–283.

58. Thorel, F., N. Damond, …, P. L. Herrera. 2011. Normal glucagon signaling and β-cell function after near-total α-cell ablation in adult mice. *Diabetes.* 60:2872–2882.

59. Hellman, B., A. Salehi, …, E. Grapengiesser. 2009. Glucose generates coincident insulin and somatostatin pulses and antisynchronous glucagon pulses from human pancreatic islets. *Endocrinology.* 150:5334–5340.

60. Hellman, B., A. Salehi, …, E. Gylfe. 2012. Isolated mouse islets respond to glucose with an initial peak of glucagon release followed by pulses of insulin and somatostatin in antisynchrony with glucagon. *Biochem. Biophys. Res. Commun.* 417:1219–1223.